Role of Adsorbed NO in N_2O Decomposition over Iron-Containing ZSM-5 Catalysts at Low Temperatures

Dmitri A. Bulushev, Albert Renken, and Lioubov Kiwi-Minsker*

Ecole Polytechnique Fédérale de Lausanne, LGRC-EPFL, CH-1015, Lausanne, Switzerland

Received: December 6, 2005; In Final Form: April 10, 2006

Transient response and temperature-programmed desorption/reaction (TPD/TPR) methods were used to study the formation of adsorbed NO_x from N_2O and its effect during N_2O decomposition to O_2 and N_2 over FeZSM-5 catalysts at temperatures below 653 K. The reaction proceeds via the atomic oxygen $(O)_{Fe}$ loading from N_2O on extraframework active Fe(II) sites followed by its recombination/desorption as the rate-limiting step. The slow formation of surface $NO_{x,ads}$ species was observed from N_2O catalyzing the N_2O decomposition. This autocatalytic effect was assigned to the formation of $NO_{2,ads}$ species from NO_{ads} and $(O)_{Fe}$ leading to facilitation of $(O)_{Fe}$ recombination/desorption. Mononitrosyl Fe^{2+}(NO) and nitro ($NO_{2,ads}$) species were found by diffuse reflectance infrared fourier transform spectroscopy (DRIFTS) in situ at 603 K when N_2O was introduced into NO-containing flow passing through the catalyst. The presence of $NO_{x,ads}$ does not inhibit the surface oxygen loading from N_2O at 523 K as observed by transient response. However, the reactivity of $(O)_{Fe}$ toward CO oxidation at low temperatures (<523 K) is drastically diminished. Surface NO_x species probably block the sites necessary for CO activation, which are in the vicinity of the loaded atomic oxygen.

1. Introduction

Development of effective catalysts for the removal of NO_x and N_2O from waste gases is an important task in the field of catalysis. The first gas is dangerous for humans, and the second one is a greenhouse gas. Iron-containing ZSM-5 zeolites are known to catalyze N_2O decomposition and selective catalytic reduction of NO_x by ammonia or hydrocarbons.

Often the N_2O and NO_x gases are present in exhaust, which contains also water vapor, oxygen, CO_2 and other gases. O_2 and CO_2 do not influence N_2O decomposition,[1−3] H_2O inhibits the reaction,[1−3] and NO and CO promote it.[2−11] Recently it was shown[9] that at low partial pressures the NO effect was stronger than the effect of CO. Evidently, more extended mechanistic studies are necessary in this field.

The N_2O decomposition to N_2 and O_2 is known to involve Fe-containing sites and proceeds via atomic surface oxygen loading from N_2O as a first step:

$$N_2O + (\ )_{Fe} \rightarrow N_2 + (O)_{Fe} \qquad (1)$$

It is important that the formed oxygen called α-oxygen possesses extremely high, unusual reactivity in benzene hydroxylation to phenol and in methane, CO and H_2 oxidation to methoxy species, CO_2 and H_2O, respectively.[12,13] However, the reactivity of the surface oxygen toward oxidation in the presence of different gases has been insufficiently studied.

Recently it was evidenced that adsorbed NO species (NO_{ads}) are formed from N_2O on the surface of iron- and copper-containing ZSM-5[2,11,14−18] via the reaction

$$N_2O \rightarrow NO_{ads} + 0.5N_2 \qquad (2)$$

Surface NO_{ads} can be further oxidized to adsorbed NO_2 species ($NO_{2,ads}$).[5,14,19,20] Formation of $NO_{x,ads}$ was found to depend on the concentration of active iron sites in zeolites, the N_2O concentration, temperature and time on stream.[18] A considerable increase of the N_2O decomposition rate upon NO introduction to the reaction mixture was reported by different studies.[4−6,8,10] In our previous publications[2,11,18] we reported that the adsorbed NO is slowly formed from N_2O and accelerates N_2O decomposition to O_2 and N_2 at low temperatures (<623 K). This increase of the reaction rate (autocatalytic behavior) was related to the facilitation of atomic oxygen recombination/desorption:

$$2(O)_{Fe} + NO_{ads} \rightarrow O_2 + 2(\ )_{Fe} + NO_{ads} \qquad (3)$$

This paper presents a detailed study of the NO_{ads} catalytic effect on the N_2O decomposition. The interaction of gaseous NO with the surface oxygen loaded from N_2O was investigated by the transient response method and the temperature-programmed desorption/reaction. The reactivity of the loaded oxygen with respect to CO oxidation was compared in the presence and without surface $NO_{x,ads}$ species.

2. Experimental Section

2.1. Catalysts. The isomorphously substituted ZSM-5 with Si/Al = 42 containing 350 ppm of Fe (ZSM-5_{350}) was synthesized via a hydrothermal route.[21] To get a higher sensitivity, a DRIFTS study was performed with a sample containing 2.1 wt % of Fe (2.1% Fe−ZSM-5). A postsynthesis iron deposition for this sample was performed with the ZSM-5_{150} sample (Fe-150 ppm, Uetikon, Switzerland) and by adsorption from an $Fe(CH_3COO)_3$ aqueous solution (0.01 M). The catalysts were activated in a He flow (50 mL (STP)/min) at 1323 K for 1 h.[22] It was shown earlier that even much more prolonged heating of ZSM-5 samples with different Fe content at 1323 K does not change the XRD pattern, a decrease of the BET surface area of only 10% was observed.[2] At the same time this thermal treatment increases several times the amount of

* To whom correspondence should be addressed. E-mail: lioubov.kiwi-minsker@epfl.ch.

10.1021/jp057104m CCC: $33.50
Published on Web 05/13/2006

active iron sites as compared to the thermal treatment in He for 1 h at 1173 K[22,23] and steaming at 823 K.[21]

The chemical composition of the catalysts was determined by atomic absorption spectroscopy (AAS) via a Shimadzu AA-6650 spectrometer after dissolution of the sample.

NO molecule probe adsorption performed on the ZSM-5_{350} and 2.1% Fe−ZSM-5 samples controlled by DRIFTS indicated the similarity of iron species able to adsorb NO.[18] The concentration of active iron sites in the ZSM-5_{350} sample is 1.9×10^{18} sites g^{-1}, corresponding to about 50% of the total concentration of iron. For the 2.1% Fe−ZSM-5 sample, the active iron site concentration is 5 times higher; however, this corresponds to only 4% of the total concentration of iron.[21]

2.2. DRIFTS in Situ Studies. A Perkin-Elmer FTIR spectrometer with a MCT detector was used for the DRIFTS experiments. The catalyst (∼0.015 g) ground in an agate mortar was placed into a cup of a SpectraTech 003-102 DRIFTS cell with CaF_2 windows. The cell was attached to a setup described earlier.[24] This setup allowed quick switching between two flows, one with pure Ar, another containing 0.5 vol % of NO in Ar. The used flow rate was 20 mL (STP)/min.

Before every run the activated catalyst was pretreated in the cell in Ar at 823 K for 60 min. DRIFT spectra taken every 0.5 min were obtained by averaging of 32 scans with a resolution of 4 cm^{-1}. A single beam spectrum of the catalyst before introduction of the NO-containing mixture into the cell at the interaction temperature was taken as a background. The contribution of the gaseous NO to the spectra was negligible. This was shown by measuring the spectra of the mixture containing 0.5 vol % NO over KBr.

An effect of N_2O on the NO adsorbed species was studied by an introduction of a mixture containing N_2O (2 vol %) in the flow of NO (0.5 vol %) passing through a catalyst at 603 K. In this experiment 10 mL of this mixture was introduced within 1 min using a gastight syringe via a septum.

2.3. Catalytic Activity Measurements. Catalytic activity measurements and temperature-programmed studies were performed with a Micromeritics AutoChem 2910 analyzer. A ThermoStar 200 (Pfeiffer Vacuum) quadrupole mass spectrometer was used for gas analysis. Calibrations were carried out with gas mixtures of known compositions. The following peaks were controlled simultaneously by the mass spectrometer: 4 (He), 18 (H_2O), 28 (N_2, N_2O), 30 (NO, N_2O), 32 (O_2), 40 (Ar), 44 (N_2O) and 46 (NO_2) *m*/*e*. The lines of the setup as well as a fused silica capillary connected to the mass-spectrometer were heated to 383 K. Sometimes, a NO_x detector (EcoPhysics CLD 822) with a sensitivity of ≥10 ppm of NO_x was used to identify the nitrogen oxides during the N_2O interaction.

The amount of catalysts placed in a quartz plug-flow reactor was equal to 0.8 g. Before every run the activated catalyst was pretreated in He (50 mL (STP)/min) at 1323 K for 1 h, then cooled to 523 K.

In transient response experiments a 2 vol % N_2O/2 vol % Ar/96 vol % He mixture was used. Argon was introduced as an inert tracer. During the temperature-programmed reaction (TPR) studies the catalyst was heated with a 10 K/min ramp. NO contact with the catalyst was performed for 5 min (0.5 vol % NO/0.5 vol % Ar/99 vol % He mixture). The total flow rates of the gas mixtures were equal to 20 mL (STP)/min. After N_2O or NO contacted the catalyst, the reactor was purged by He for 10 min, and temperature-programmed desorption (TPD) was performed in He (20 mL (STP)/min) with a 30 K/min ramp. The amounts of oxygen and NO evolved in TPD runs were determined by integration of the measured curves.

TABLE 1: Transient Response Experiments Performed with the ZSM-5_{350} Sample

transient response experiments at 523 K	TPD	TPR	CO at 473 K followed by TPD in He
1. N_2O, 5 min	+	+	+
2. N_2O, 65 min	+	+	+
3. $N_2O \rightarrow He \rightarrow NO$	+	−	−
4. $N_2O \rightarrow He \rightarrow NO \rightarrow He \rightarrow N_2O$	+	−	−
5. NO, 5 min	+	−	−
6. $NO \rightarrow He \rightarrow N_2O$	+	+	+

[a] The experiments with NO and N_2O were performed for 5 min except of experiment 2.

Reactivity of the oxygen loaded from N_2O on the ZSM-5_{350} sample (0.5 g) was characterized by passing CO (3 vol % in He, 20 mL (STP)/min) at 473 K for 10 min over the catalyst and determination of the CO_2 formed. Afterward, a TPD run in He was performed. Gas purities were higher than 99.998% except of NO, which was >99.9%. The experiments accomplished are summarized in Table 1. After every treatment before TPD, TPR or CO oxidation the reactor was purged by He. The same numeration of experiments as in Table 1 was used for the curves in the figures.

3. Results

3.1. N_2O Decomposition to O_2 and N_2 in TPR. Interaction of N_2O with the ZSM-5_{350} catalyst was performed at 523 K for 5 and 65 min as well as after pretreatment of the catalyst with NO (experiments 1, 2 and 6) to understand the role of the pretreatment on N_2O decomposition. Nitrogen was the only product of the N_2O interaction with Fe−ZSM-5 at 523 K (Figure 2). The influence of the different catalyst treatment was followed by temperature-programmed reaction (TPR) (Figure 1). The oxygen monitored during the temperature-programmed N_2O decomposition is shown in Figure 1. N_2O decomposition leading to O_2 production was observed to start at around 573 K.

The temperature dependence of the oxygen evolution (N_2O conversion) shows an up to 2 times higher conversion if the catalyst is treated for 65 min than for 5 min before the TPR (curve 2 and 1, Figure 1). It is interesting that the same conversion as after 65 min in N_2O was obtained if the N_2O interaction was performed for 5 min, but after NO preadsorption on the catalyst (curve 6, Figure 1).

Recently we reported[2,11] that a steady-state N_2O decomposition in an open system at the studied temperatures is only attained after more than 1 h. In accordance, the presented conversion-temperature dependence after 5 min in N_2O (curve 1, Figure 1) corresponds to the transient, but not to the steady-state behavior of the catalyst.

Gas-phase NO was observed during TPR at high temperatures (623−773 K) (Figure 1, inset). The concentration of NO was higher after 65 min pretreatment in N_2O (curve 2, Figure 1, inset) than after 5 min (curve 1, Figure 1, inset) and almost equal to the one obtained after the NO preadsorption followed by the 5 min N_2O interaction (curve 6, Figure 1, inset).

Thus, it is concluded that there was a formation and accumulation of adsorbed NO on the zeolite during N_2O pretreatment. The results reported in Figure 1 indicate that the zeolite activity in N_2O decomposition is dependent on the amount of accumulated NO. The data show that the higher the amount of adsorbed NO, the higher is the zeolite activity for N_2O decomposition.

3.2. Oxygen Loading on Iron Sites from N_2O. To explore if an interaction of NO with the oxygen loaded from N_2O takes place and to check how stable are the surface species, the N_2O

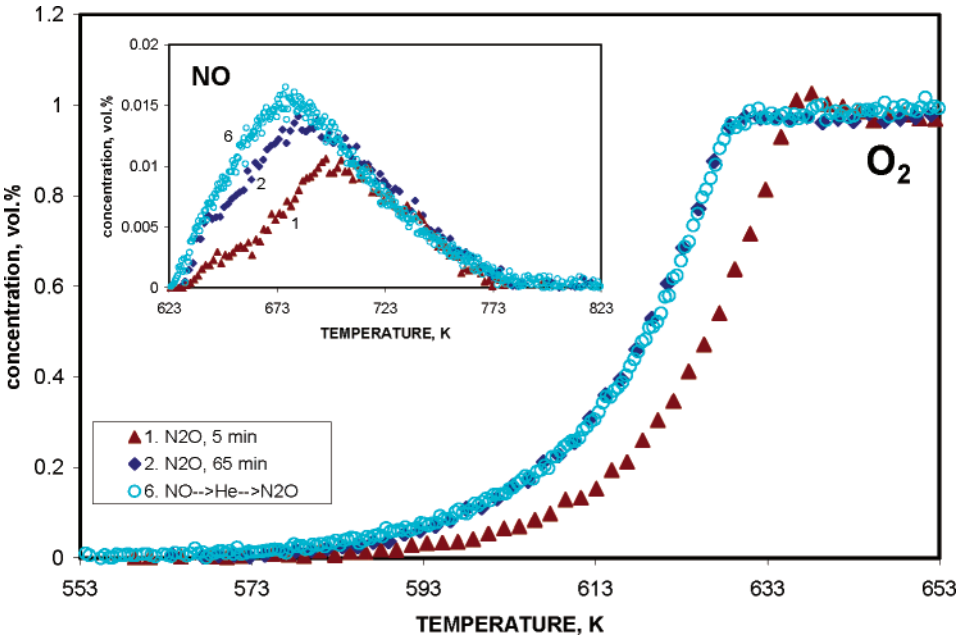

Figure 1. Oxygen evolution during temperature-programmed reaction (TPR) of N_2O decomposition (2 vol %) over the ZSM-5_{350} catalyst after (1) 5 min of the N_2O interaction at 523 K, (2) 65 min of the N_2O interaction at 523 K, (6) NO preadsorption (0.5 vol % NO, 5 min) and 5 min of the N_2O interaction at 523 K. Inset: NO evolution during TPR.

interaction with the ZSM-5_{350} catalyst followed by TPD was performed after different catalyst pretreatments (NO (0.5 vol % NO, 5 min) or N_2O (2 vol %, 5 min) followed by NO (0.5 vol % NO, 5 min)) at 523 K.

During the NO interaction with the catalyst at 523 K no formation of gaseous N_2O, N_2, NO_2 or O_2 was observed independently on the catalyst pretreatment. NO was adsorbed on the zeolite in reversible and irreversible forms. The reversibly adsorbed NO was removed from the surface during the He purge for 10 min.

During the N_2O interaction with the catalyst at 523 K only nitrogen was evolved (Figure 2a) and no other gaseous products were observed. The reversible adsorption of N_2O was also detected. Its concentration was determined as the difference between the Ar curve and the sum of the N_2O with N_2 curves (Figure 2b).

Atomic oxygen was loaded from N_2O on iron sites as reported earlier.[2,12,22,23,25] The loading takes place according to reaction 1. The total amount of nitrogen formed during the interaction of N_2O with the ZSM-5 catalyst after different pretreatments was determined and shown in Figure 2a. It is seen that the amount of N_2 was ca. 1.5 times higher after preadsorbing NO (Figure 2a, curves 4 and 6) as compared to the experiment without NO preadsorption (Figure 2a, curve 1). This suggests that: 1) there is no competition of the loaded oxygen and adsorbed NO for the same sites, 2) the adsorbed NO interacts with the atomic oxygen loaded from N_2O

$$(O)_{Fe} + NO_{ads} \rightarrow NO_{2,ads} + (\ )_{Fe} \qquad (4)$$

As a result of this interaction, the active sites $(\ )_{Fe}$ are liberated, providing an additional oxygen loading from N_2O according to reaction 1. However, the N_2 response shapes were different depending on the sequence of catalyst pretreatment: (He → NO → He) or (He → N_2O → He → NO → He) (Figure 2a, curves 6, 4). This may be due to different concentrations and concentration ratios of adsorbed NO and NO_x species after these pretreatments, as will be shown below.

It is interesting that the effect of the adsorbed NO_x species on the concentration of reversibly adsorbed N_2O was negligible (Figure 2b). This indicates that adsorbed NO/NO_x species do not block the sites responsible for the reversible N_2O adsorption. To shed some light into the features of the NO interaction with the oxygen loaded on ZSM-5_{350} catalyst from N_2O, TPD experiments were performed after different catalyst pretreatments.

3.3. Temperature-Programmed Desorption. Oxygen and NO were evolved during the temperature-programmed desorption experiments after the N_2O interaction with the zeolite at 523 K giving the observed desorption peaks at around 630−670 and 700 K, respectively (Figure 3). The amount of NO accumulated on the surface increased almost 1 order of magnitude by increasing the time of N_2O pretreatment from 5 to 65 min (Figure 3b). The increase of the adsorbed NO concentration caused a ∼30 K shift of the oxygen TPD peak to lower temperatures, indicating easier oxygen desorption. It is seen also that the desorption of oxygen (Figure 3a) is observed in the same temperature range as the decomposition of N_2O to O_2 and N_2 under TPR conditions (Figure 1). Adsorbed NO_x species facilitate the oxygen desorption (Figure 3a) as well as N_2O decomposition (Figure 1). This confirms that the oxygen recombination/desorption step (reaction 3) is rate determining during N_2O decomposition to O_2 and N_2 at low temperatures (<623K).

The amount of the evolved oxygen in TPD corresponding to the surface concentration of active iron sites was found to be 1.9×10^{18} atoms g^{-1} after 5 min of N_2O interaction. A slight increase of this value after 65 min pretreatment in N_2O to 2.3×10^{18} atoms g^{-1} is probably due to the contribution of the decomposition of $NO_{x,ads}$ species formed from N_2O in larger concentration than after 5 min.

A TPD pattern obtained after NO adsorption on the zeolite is shown in Figure 4, exp 5. The irreversibly adsorbed NO is responsible for a TPD peak with a maximum at 688 K, confirming strong NO adsorption on the FeZSM-5 sample. A small oxygen evolution at 723 K was reproducibly observed during TPD after NO adsorption. The total amount of the desorbed NO is close to the amount of active iron sites determined by TPD of oxygen, indicating that the same Fe(II)

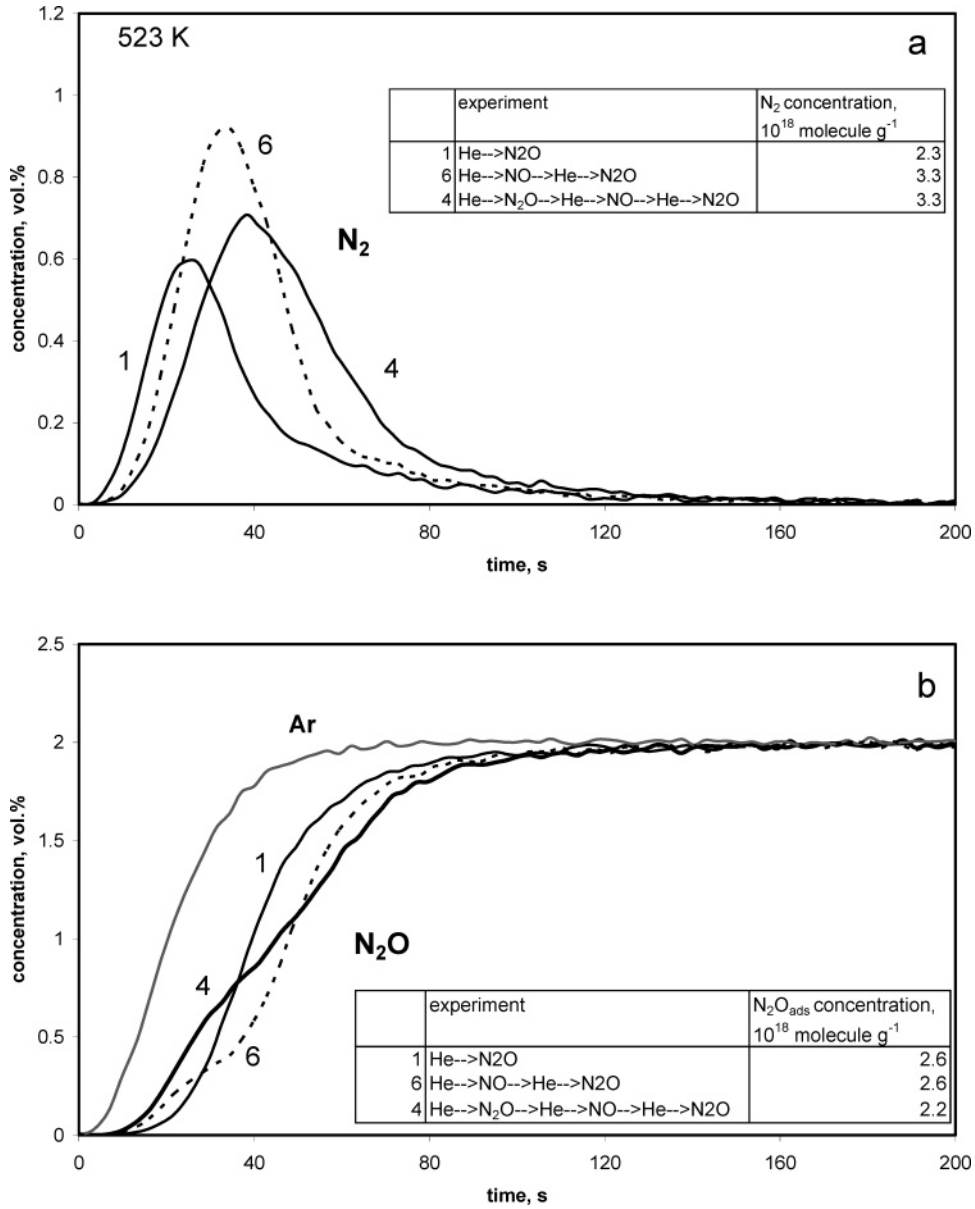

Figure 2. Response curves of N_2 (a) and N_2O (b) obtained at 523 K during introduction of the 2 vol % N_2O, 2 vol % Ar mixture in He on the ZSM-5_{350} catalyst (1) treated in He at 1323 K 1 h, (6) after (1) treated with NO (0.5 vol %, 5 min) and then with He for 10 min at 523 K, (4) after (1) treated with N_2O (2 vol %, 5 min), with He for 10 min, with NO (0.5 vol %, 5 min), and then with He for 10 min at 523 K. Inert tracer: Ar response shown for comparison.

species are responsible for the NO adsorption and oxygen loading from N_2O.

After the N_2O interaction with the catalyst containing irreversibly preadsorbed NO (Figure 2, curves 6), a large O_2 peak at 631 K appeared in TPD (Figure 4, exp 6) contrary to the experiment without the N_2O interaction (Figure 4, exp 5). The oxygen peak can be decomposed into two peaks: one at 723 K, as observed after the NO interaction (Figure 4, exp 5), and another at 631 K, which is very similar to the one obtained after 65 min of the N_2O interaction (Figure 3a, curve 2). This peak was assigned to the loaded oxygen from N_2O. The oxygen peak (Figure 4, exp 6) was slightly shifted to lower temperatures than after 65 min of the N_2O interaction (Figure 3a, curve 2). This can be explained by the 1.5 times higher amount of NO adsorbed on the catalyst in the experiment with the NO preadsorption compared to NO formed from N_2O during the 65 min of interaction. The amount of oxygen desorbed was not decreased after the NO preadsorption in accordance with the oxygen loading results (Figure 2a).

TPD experiments in which NO interacted with the catalyst after the oxygen loading from N_2O were performed also. It is important that the desorbed NO amount after the oxygen loading doubled (Figure 5, exp 3), as compared to the amounts evolved after NO adsorption (Figure 4, exp 5). This could indicate a consumption of oxygen by NO with the formation of adsorbed NO_x species (reaction 4), which could be located not directly on iron sites. Thus, the released iron sites can adsorb NO, strongly providing the doubled increase in the NO + NO_x species concentration. The same amounts of nitrogen were evolved during the N_2O interaction with the catalyst pretreated consequently by N_2O and NO (Figure 2, exp 4) and only NO (Figure 2, exp 6), showing that the same concentrations of adsorbed NO species were present in both cases.

Oxygen evolution was clearly observed during the TPD runs and this is reported in Figure 5, exp 3. The shape and T_{max} of the O_2 peak differed considerably from the ones obtained after oxygen loading from N_2O (Figure 3a). The values of T_{max} for the NO and O_2 peaks were similar (Figure 5, exp 3). This

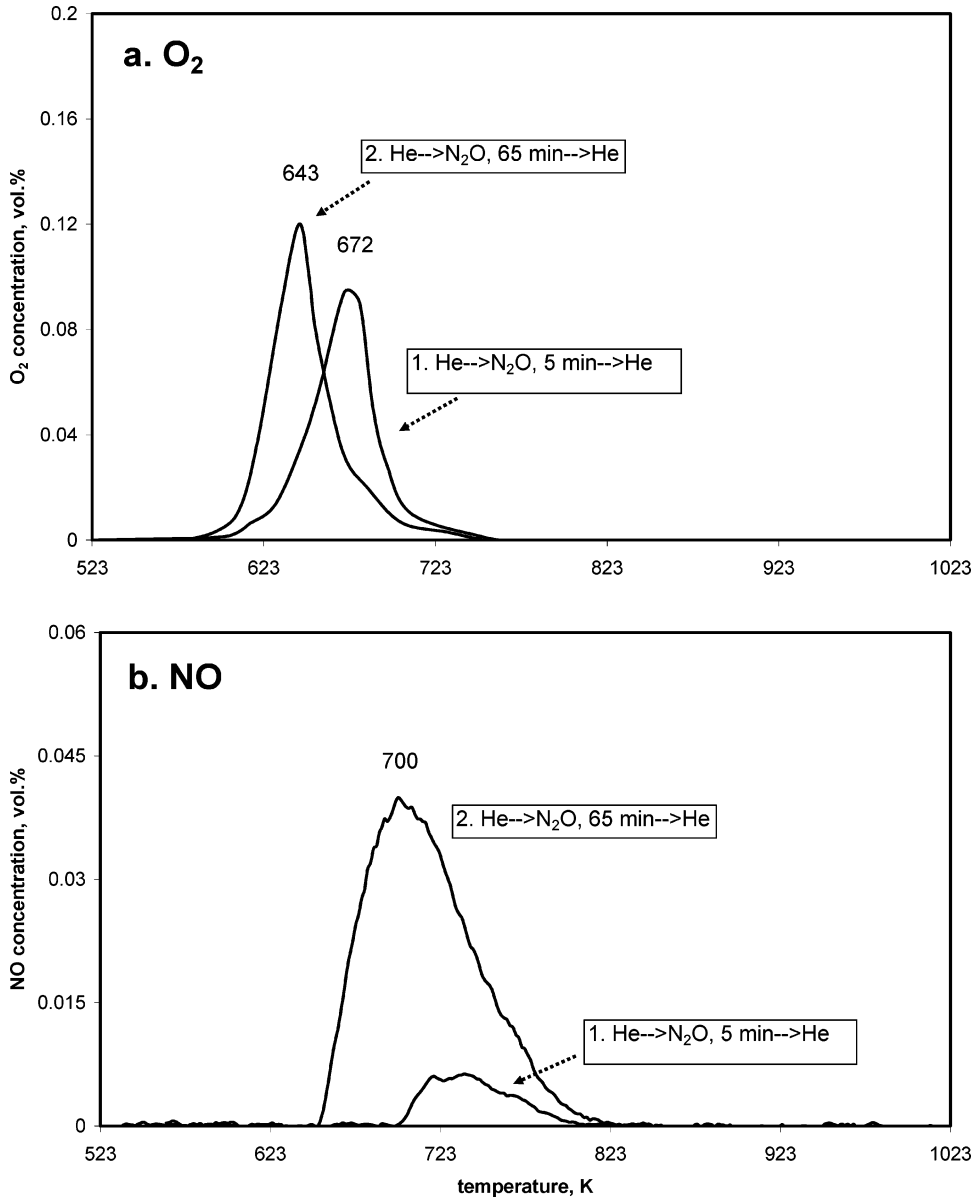

Figure 3. TPD profiles of oxygen (a) and NO (b) after 5 (1) and 65 (2) min of the N_2O interaction (2 vol %) with the ZSM-5_{350} catalyst.

indicates that the oxygen loaded from N_2O was completely consumed in the reaction with NO forming $NO_{2,ads}$ (reaction 4). $NO_{2,ads}$ probably decomposed, giving simultaneously NO and O_2 in TPD according to the reaction:

$$NO_{2,ads} \rightarrow 0.5O_2 + NO \quad (5)$$

Additionally, desorption of NO

$$NO_{ads} \rightarrow NO \quad (6)$$

can contribute to the NO TPD profile. Gaseous NO_2 was not observed.

To check whether the adsorbed NO/NO_x species block the sites for oxygen loading from N_2O, the N_2O introduction was performed after N_2O followed by NO interaction (He → N_2O → He → NO, Figure 2, exp 6). It is seen that N_2O easily loaded atomic oxygen in the presence of $NO_{x,ads}$ species. The TPD profile after this interaction is shown in Figure 5, exp 4. Again, the oxygen peak with a maximum at 641 K and a similar height as in the previous runs (Figure 3a, Figure 4, exp 6) was observed in the TPD profile, confirming reaction 3. Deconvolution of the oxygen curve (Figure 5, exp 4) shows that the $NO_{x,ads}$ decomposition (Figure 5, exp 3) contributes similarly to the TPD profile. Thus, the $NO_{x,ads}$ species as well as the adsorbed NO do not block the sites for oxygen loading from N_2O. Adsorbed NO is converted to the adsorbed NO_x species during the oxygen loading from N_2O. Decomposition of the $NO_{x,ads}$ species gives another type of oxygen evolving simultaneously with NO at 688 K (Figure 5, exp 3), as compared to the evolution of oxygen loaded from N_2O assigned to the 641 K peak (Figure 5, exp 4).

Adsorbed NO/NO_x species always resulted in facilitated oxygen desorption from the iron sites. The oxygen peak was shifted to the lower temperature region as compared to the peak after the oxygen loading on the NO free surface (Figure 3a, curve 1). DRIFT spectroscopy was used to characterize the nature of the adsorbed species formed during the NO/N_2O interaction with the 2.1% Fe−ZSM-5 catalyst.

3.4. DRIFTS in Situ Study. A spectrum of adsorbed species formed during the interaction of NO (0.5 vol %) with the 2.1% Fe−ZSM-5 catalyst at 603 K is shown in Figure 6 (before N_2O interaction). The main peak of adsorbed NO (1883 cm^{-1}) could be assigned to mononitrosyl species associated with Fe(II). The

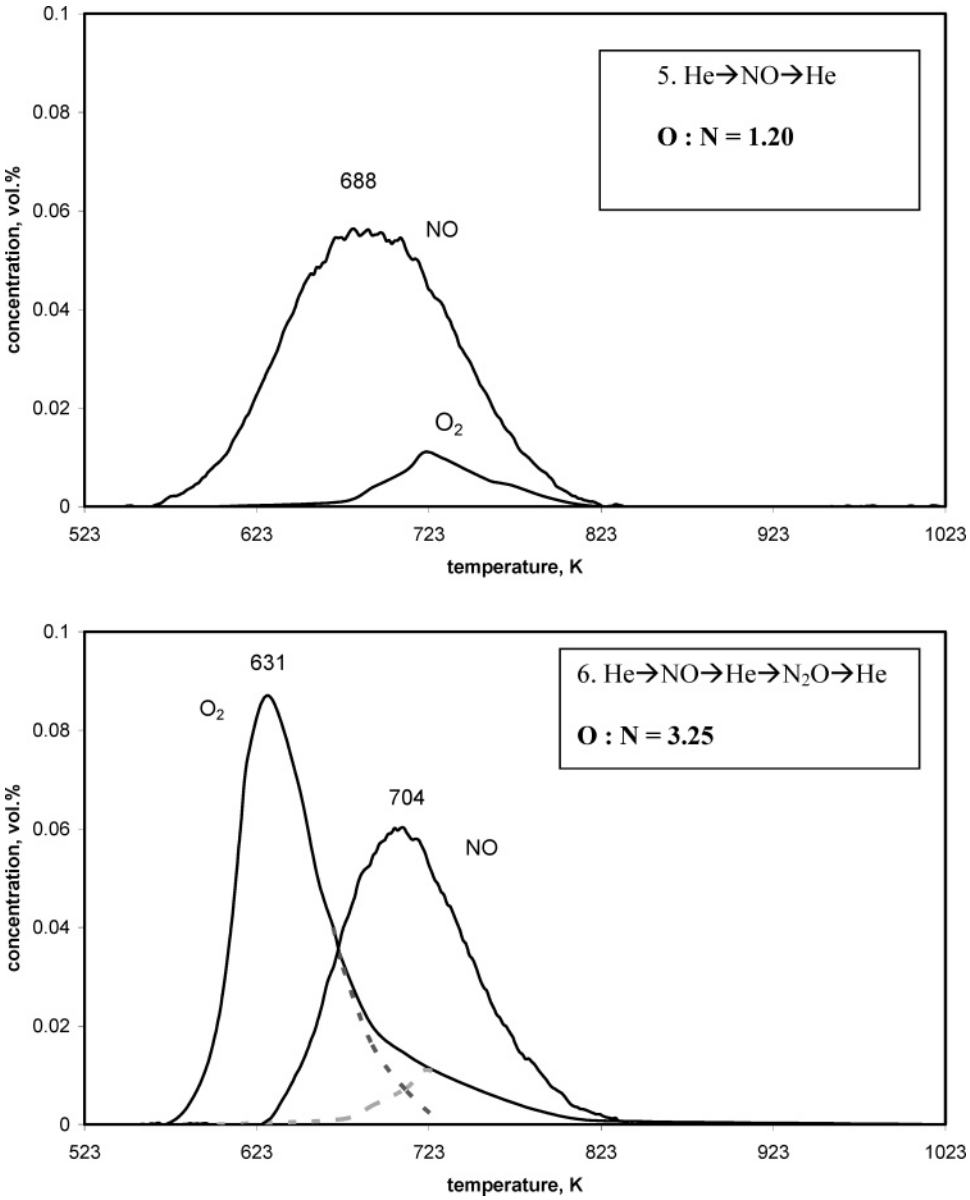

Figure 4. TPD profiles obtained (5) after interaction of NO (0.5 vol %, 5 min at 523 K) with the ZSM-5_{350} catalyst and (6) after (5) followed by 5 min of the interaction with N_2O (2 vol %, 5 min) at 523 K.

asymmetric shape of the peak indicates at least two Fe(II) species in accordance with NO adsorption at room temperature.[18] A very weak peak of adsorbed NO^+ species present in cation-exchange positions of zeolite (2124 cm^{-1}) is also observed.

After 6 min of the NO interaction 10 mL of the 2 vol % N_2O-containing mixture were added to the NO flow by a syringe. The bands of gaseous N_2O are clearly seen (Figure 6). The mononitrosyl band decreased while the peak at 1628 cm^{-1} appeared. This band is assigned tentatively to adsorbed nitro species ($NO_{2,ads}$).[6,14,19,20,26−28] This adsorbed NO_2 could be formed in the reaction of NO with the oxygen loaded from N_2O on iron sites (reaction 4). Simultaneously, the intensity of the mononitrosyl species (1883 cm^{-1}) decreased. When the N_2O introduction was finished, the peak of adsorbed NO_2 disappeared and the adsorbed NO band reached the intensity observed before the N_2O introduction.

Thus, the formation of adsorbed NO_2 (reaction 4) is detected and high thermal stability of adsorbed NO/NO_x species in conditions of N_2O decomposition are confirmed in accordance with the TPD data (Figures 3−5). It was interesting to test the reactivity of the oxygen loaded from N_2O in the presence of $NO_{x,ads}$ species and without them.

3.5. Oxygen Reactivity toward CO Oxidation. The reactivity of oxygen loaded from N_2O was measured in CO (3 vol %) oxidation to CO_2 at 473 K. The comparison was performed after three different pretreatments (exp 1, 2, 6), which resulted in a strong oxygen peak in TPD (Figure 3a, curve 1 (NO_x free surface), Figure 3a, curve 2, and Figure 4, exp 6 (NO_x-containing surface)). The NO_x free surface was prepared by oxygen loading from N_2O during 5 min at 523 K followed by the He purge. To prepare $NO_{x,ads}$-containing surfaces, the N_2O interaction was performed for 65 min as well as for 5 min after the NO preadsorption (5 min) followed by the He purge. The reaction of the $NO_{x,ads}$ formation from N_2O on Fe−ZSM-5 catalysts is slow.[18] The N_2O interaction for 65 min at 523 K provides only 50% coverage by $NO_{x,ads}$ from the maximal amount as is seen from the TPD profiles (Figure 3b, curve 2 and Figure 4, exp 5).

In the case of the NO_x free surface, intensive formation of CO_2 was observed and finished within 4 min (Figure 7, exp 1) due to the consumption of the reactive oxygen loaded from N_2O.

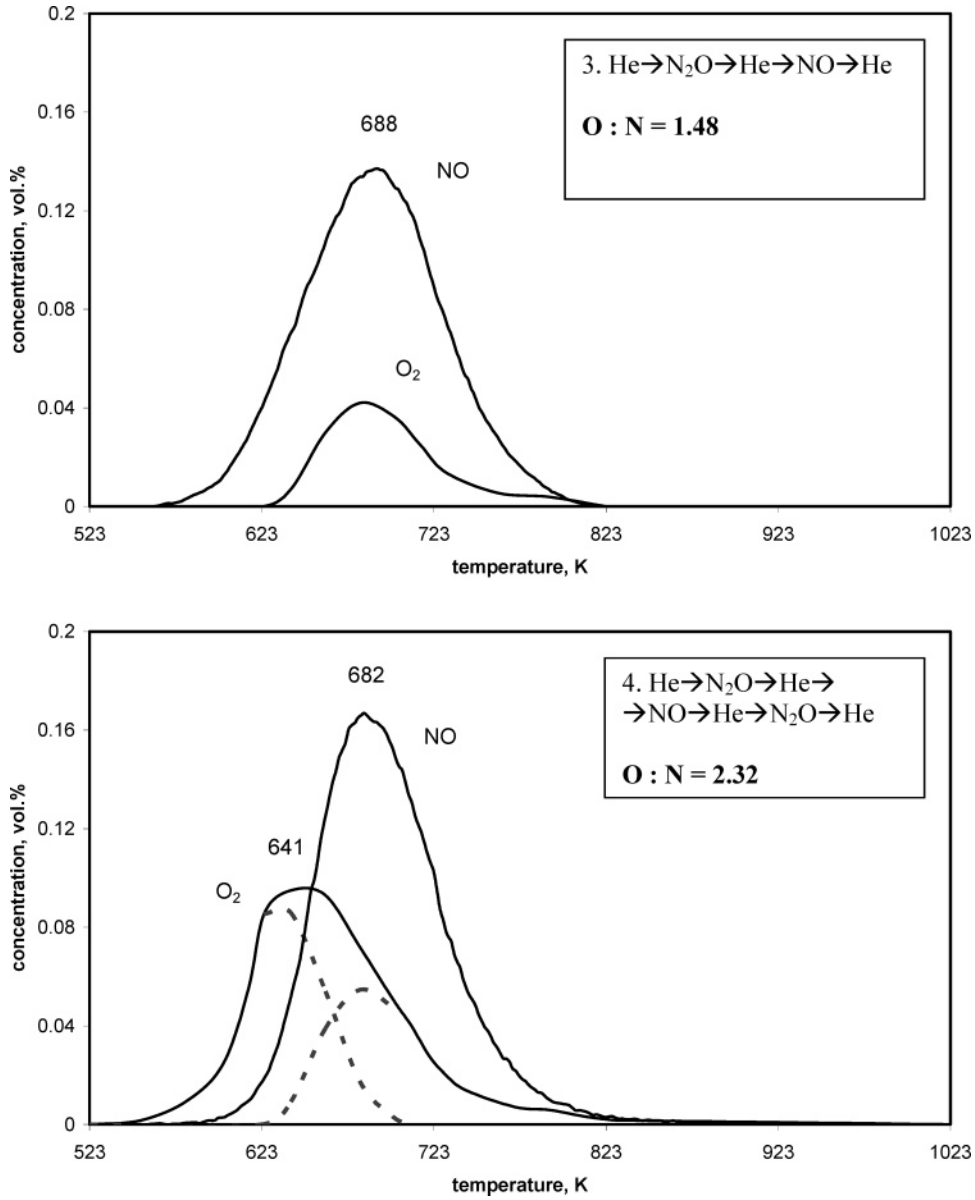

Figure 5. TPD profiles obtained (3) after consecutive interaction of N_2O (2 vol %, 5 min at 523 K) and NO (0.5 vol %, 5 min at 523 K) with the ZSM-5_{350} catalyst, (4) after (3) followed by interaction with N_2O (2 vol %, 5 min) at 523 K.

No oxygen and CO_2 was observed in TPD after the CO interaction. This shows that the oxygen loaded from N_2O giving a peak at 672 K in TPD (Figure 3a, curve 1) is very reactive in the absence of adsorbed NO_x species.

In contrast to the NO_x free surface, the oxygen on the surface saturated with $NO_{x,ads}$ was found to be inactive with respect to CO oxidation (Figure 7, exp 6). Neither CO_2 nor NO evolution was observed at 473 K during the CO interaction. TPD profiles of NO and oxygen after the interaction were similar to the ones observed without CO interaction (Figure 4, exp 6).

The amount of CO_2 formed on the surface partially covered by adsorbed NO_x species formed during 65 min interaction with N_2O was decreased twice as compared to the amount formed on the NO_x free surface (Figure 7, exp 2 and exp 1). It is important that the decrease of the amount of formed CO_2 corresponds to the amount of $NO_{x,ads}$ species.

Hence the same $NO_{x,ads}$ species are formed during 65 min of the N_2O interaction and during 5 min of the N_2O interaction performed after the NO pretreatment of the sample. All these results could indicate that the oxygen evolving at 630−640 K is involved in nonreactive $NO_{x,ads}$ species or that some sites necessary for CO activation before the interaction with the loaded oxygen are occupied by $NO_{x,ads}$ species.

4. Discussion

4.1. Oxygen Loading. Extraframework Fe(II) sites in ZSM-5 catalysts are considered as active sites for the formation of active oxygen species from N_2O. The nuclearity of these sites as well as the necessity of Al cation in the vicinity of iron is a matter of discussion: isolated,[29−31] binuclear,[14,23,32,33] oligonuclear[30,34,35] sites are proposed to be active in N_2O decomposition.

The loading of oxygen on iron sites from N_2O probably takes place via a reversibly adsorbed N_2O (N_2O_{ads}) present in equilibrium with gas-phase N_2O.[11] The atomic oxygen $(O)_{Fe}$ loaded from N_2O on active iron sites was theoretically proved to be an anion-radical type in ferryl species $[Fe^{3+}O^{-}]$ present in the specific zeolite environment.[36] This oxygen desorbs at 600−670 K after the zeolite preloading by atomic oxygen during the N_2O interaction with the catalysts at 523 K.[12,18,21,23,25] The anion−radical oxygen possesses high reactivity oxidizing CO to CO_2 at 473 K (Figure 7, exp 1). The activation of CO in the vicinity of $(O)_{Fe}$ is probably necessary.

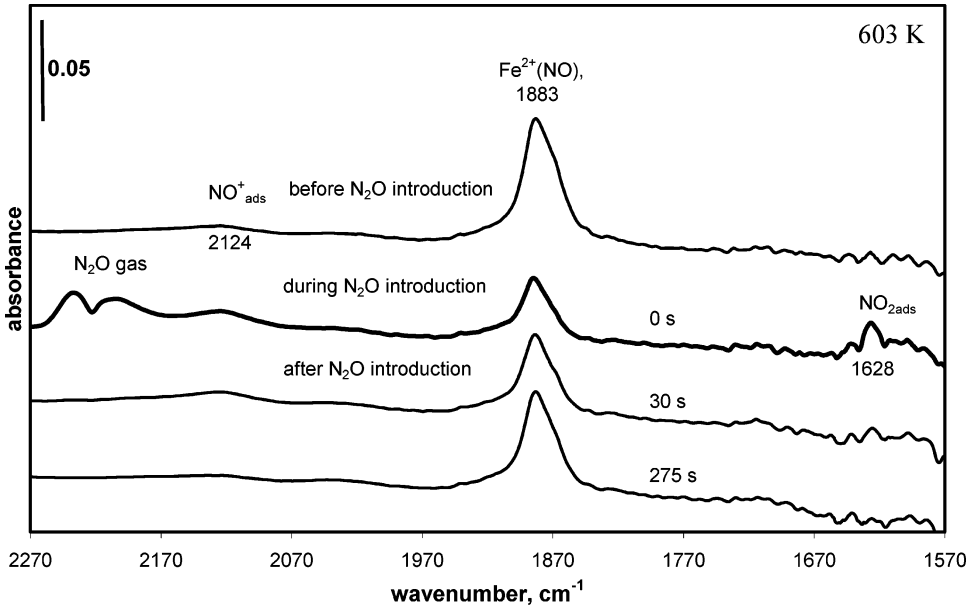

Figure 6. DRIFT spectra of the 2.1% Fe−ZSM-5_{150} sample showing an effect of the N_2O introduction (via a syringe) in the NO-containing flow (0.5 vol %) passing through the catalyst at 603 K.

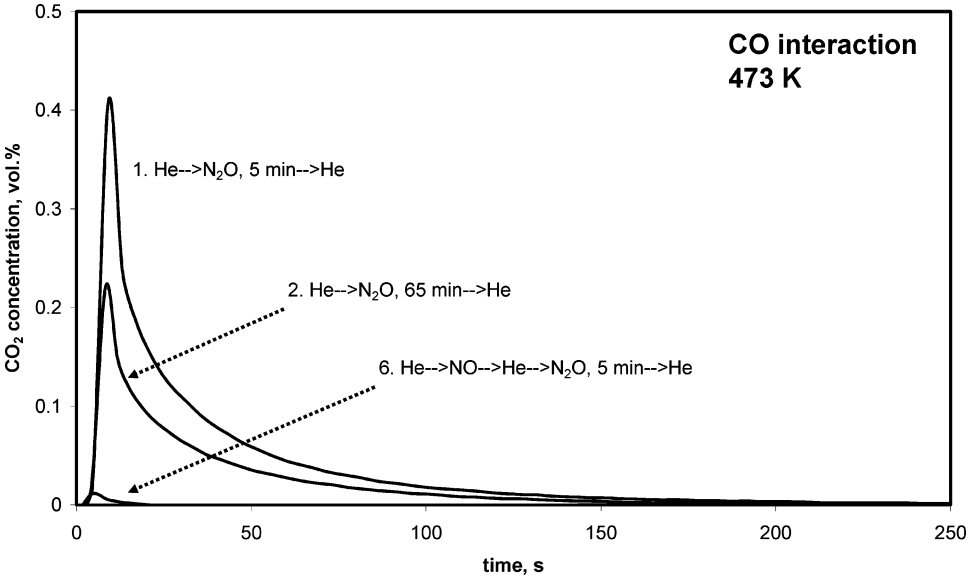

Figure 7. CO_2 evolution during CO interaction (3 vol %) with the ZSM-5_{350} catalyst (0.5 g) at 473 K after oxygen loading via the N_2O interaction (2 vol %) at 523 K for (1) 5 min and (2) 65 min and (6) 5 min after the pretreatment in NO (0.5 vol %, 5 min at 523 K).

4.2. Adsorbed NO_x Formation. Adsorbed NO_x species are formed from N_2O during contact with Fe−ZSM-5 catalysts at low temperatures (<653 K). The formation of these species is slow and takes place for 60 min after loading of the active iron sites with atomic oxygen at 523 K (Figure 2a, curve 1).[2,18] This shows that the NO formation from N_2O (reaction 2) includes at least two steps: the atomic oxygen loading (reaction 1) and interaction of the loaded oxygen with N_2O, which probably takes place via dimer $(NO)_2$ species[33]

$$N_2O + (O)_{Fe} \rightarrow 2NO_{ads} + (\ )_{Fe} \qquad (7)$$

Additionally, the formation of adsorbed NO is followed by its easy oxidation to $NO_{2,ads}$. Reaction 1 is much faster than reaction 7, thus keeping iron sites completely covered by oxygen at 523 K. It should be mentioned also that the step (7) is the reverse to the step of N_2O and adsorbed oxygen formation from NO over Cu−ZSM-5 catalysts followed by N_2O decomposition to O_2 and N_2.[37]

The DRIFT spectra of adsorbed NO at 603 K were mainly presented by the species responsible for the bands at around 1860−1900 cm^{-1} (Figure 6). These species possess high thermal stability, indicating strong interaction of NO with iron sites in activated samples. Generally, Fe(II) cations adsorb NO more strongly than the Fe(III) ones. The assignment of the iron sites to Fe(II) involved in bi- and oligonuclear iron species associated with aluminum extraframework cations[20] seems preferable.

It is important that adsorbed NO does not block the iron sites for oxygen loading (Figure 2a and Figure 4) and sites for N_2O reversible adsorption (Figure 2b). NO interacts with N_2O or oxygen loaded from N_2O forming adsorbed $NO_{2,ads}$ species, which could be located in the vicinity of the active iron sites. The surface reaction

$$2N_2O + NO_{ads} + (\ )_{Fe} \rightarrow NO_{2,ads} + 2N_2 + (O)_{Fe} \qquad (8)$$

which is not elementary could take place. Gaseous NO_2 was not observed in the present study. Adsorbed NO_2 was found

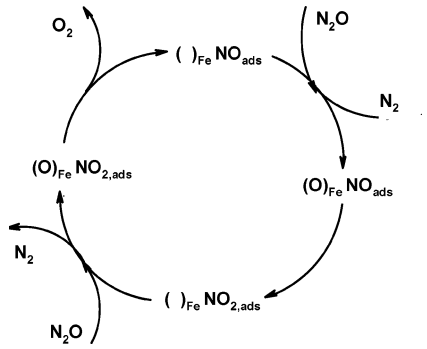

Figure 8. Schematic presentation of oxygen recombination/desorption catalyzed by $NO_{x,ads}$.

directly by DRIFTS on FeZSM-5 during the simultaneous NO and N_2O introduction at 603 K (Figure 6).

4.3. Oxygen Desorption. We showed earlier[2,11] that an accumulation of adsorbed NO_x species from N_2O affected considerably the dynamics of the N_2O decomposition to O_2 and N_2 at low temperatures (<653 K) providing a slow increase of the reaction rate with time until a steady-state was reached. Direct introduction of an NO pulse to the reaction mixture resulted in an immediate attainment of the same steady state.[2]

The comparison of the oxygen curves obtained during TPD (Figure 3a) and TPR (Figure 1) showed that the oxygen desorption is the rate-determining step in N_2O decomposition. The oxygen desorption was easier when adsorbed NO_x species were present on the surface, resulting in a shift of the oxygen evolution curves to lower temperatures. Direct participation of adsorbed NO_x in desorption of oxygen could be a reason. The formed $NO_{x,ads}$ probably interacts with the oxygen loaded on iron sites from N_2O, providing faster oxygen desorption:

$$NO_{2,ads} + (O)_{Fe} \rightarrow O_2 + NO_{ads} + (\ )_{Fe} \qquad (9)$$

releasing adsorbed NO, which is thus a cocatalyst for the N_2O decomposition to O_2 and N_2 at temperatures <653 K. A catalytic cycle of N_2O decomposition in the presence of $NO_{x,ads}$ species is shown in Figure 8. Quite similar mechanisms explaining facilitated oxygen desorption were considered earlier.[5,10,11]

The facilitation of oxygen desorption by NO was also reported for Cu−ZSM-5 catalysts.[37] The effect was assigned to more easy decomposition of the formed nitrate species than the oxygen recombination/desorption in the absence of NO. A similar explanation was proposed for increased N_2O decomposition over Fe−ZSM-5 zeolites in the presence of small amounts of NO in the gas phase.[8] A nitrate−nitrite redox cycle was also discussed for the Fe−ZSM-5 catalysts to explain a light-off behavior of N_2O decomposition.[38] It should be mentioned that nitrate species (1570−1580 cm^{-1}) were not detected in the present study by DRIFTS (Figure 6) as well as in another study.[6] The intensity of the nitrates bands observed in some studies[14,28] is much weaker than the one of adsorbed nitro species ($NO_{2,ads}$).

The nitrate species decomposition on Cu−ZSM-5 is normally accompanied by simultaneous evolution of NO and O_2 in TPD.[37] During the N_2O decomposition over Fe−ZSM-5 catalysts at low temperatures (<623 K) no NO is observed in the gas phase (Figure 1). It is important that oxygen is evolved earlier than NO during the TPD after the N_2O interaction with the NO_x-containing surface (Figure 4, exp 6 and Figure 5, exp 4) showing that evolution of oxygen and NO takes place from decomposition of different surface species. This is in agreement with the TAP reactor pump−probe experiments where the oxygen peak was observed during the N_2O pulse and became

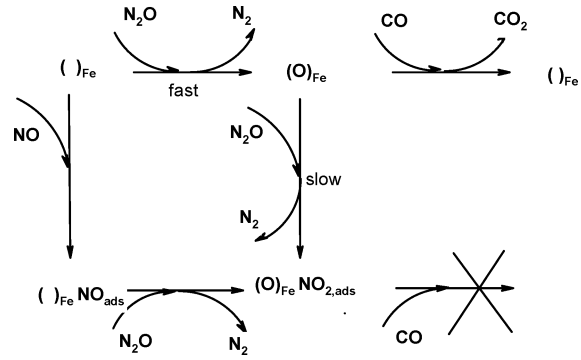

Figure 9. Schematic presentation of the influence of $NO_{x,ads}$ on the $(O)_{Fe}$ reactivity for CO oxidation.

much sharper if NO was pulsed.[5] Therefore we assign the TPD patterns observed for Fe−ZSM-5 catalysts to desorption of oxygen facilitated by $NO_{x,ads}$ species (reaction 9) and not to the decomposition of nitrate species.

4.4. Oxygen Reactivity. It is interesting that the presence of adsorbed NO/NO_x species does not suppress the oxygen loading from N_2O on active iron sites and N_2O decomposition, but it affects strongly the reactivity of the loaded oxygen with respect to CO. The oxygen became completely inactive in CO oxidation if the surface was saturated with NO before the N_2O interaction (Figure 7). The concentration of the reactive oxygen decreased proportionally to the concentration of the $NO_{x,ads}$ species formed from N_2O.

The results are schematically summarized in Figure 9. Generally, the long time interaction of N_2O with the catalyst leads to the same surface composition as after the NO interaction followed by the short time N_2O interaction. This surface composition is not reactive in CO oxidation. This is important for correct interpretation of experimental results and understanding of the oxygen reactivity in Fe−ZSM-5 zeolites.

The obtained results are in line with the recently published data that even small amounts of NO can inhibit CO oxidation by N_2O.[9] The activity in N_2O decomposition in that case approached the activity obtained for the binary N_2O + NO system. This could be understood in the frame of the adsorption strength of reactant (CO, NO). CO is known to be adsorbed less strongly than NO on iron-containing catalysts. Additionally, stable $NO_{x,ads}$ species can be formed in the latter case. Hence, adsorbed NO_x species can occupy the sites necessary for CO adsorption/activation in the vicinity of the loaded atomic oxygen.

Similarly, an inhibition of benzene hydroxylation by N_2O could be expected by $NO_{x,ads}$ species at low temperatures as the benzene adsorption is weaker than the NO_x one. Thus the atomic oxygen loading from N_2O on iron sites is not sufficient for CO oxidation. The ability of the active sites in FeZSM-5 zeolites to activate a reactant may also be an important feature leading to the observed specific catalytic properties.

5. Conclusions

Autocatalytic behavior during the N_2O decomposition to O_2 and N_2 at low temperatures (<653 K) was assigned to the surface $NO_{x,ads}$ species. $NO_{x,ads}$ species are formed from N_2O and accumulated slowly until steady-state surface composition was reached.[11] Small amounts of adsorbed $NO_{x,ads}$ accelerate N_2O decomposition. Oxygen desorption is the rate-determining step of N_2O decomposition. Adsorbed NO interacts with the oxygen loaded from N_2O forming adsorbed NO_2 species, which do not block the sites for reversible adsorption of N_2O and

oxygen loading from N_2O but facilitate oxygen recombination/desorption probably due to an easier oxygen transfer.

However, the oxygen loaded on the surface saturated with the $NO_{x,ads}$ species is not reactive with respect to CO oxidation to CO_2. This is in contrast to the oxygen loaded on the $NO_{x,ads}$ free surface, which is very active in CO oxidation even at 473 K. Surface $NO_{x,ads}$ species probably block the sites necessary for CO activation, which may be in the vicinity of the loaded oxygen. Hence, the ability to activate a substrate is a very important feature of Fe−ZSM-5 catalysts responsible for their high activity observed in oxidation reactions by N_2O.

Acknowledgment. We thank the Swiss Science Foundation for the financial support.

References and Notes

(1) El-Malki, E. M.; van Santen, R. A.; Sachtler, W. M. H. *Microporous Mesoporous Mater.* **2000**, *35*−*6*, 235.
(2) Bulushev, D. A.; Kiwi-Minsker, L.; Renken, A. *J. Catal.* **2004**, *222*, 389.
(3) Perez-Ramirez, J.; Kapteijn, F.; Mul, G.; Xu, X. D.; Moulijn, J. A. *Catal. Today* **2002**, *76*, 55.
(4) Kapteijn, F.; Marban, G.; RodriguezMirasol, J.; Moulijn, J. A. *J. Catal.* **1997**, *167*, 256.
(5) Perez-Ramirez, J.; Kapteijn, F.; Mul, G.; Moulijn, J. A. *J. Catal.* **2002**, *208*, 211.
(6) Mul, G.; Perez-Ramirez, J.; Kapteijn, F.; Moulijn, J. A. *Catal. Lett.* **2001**, *77*, 7.
(7) Sang, C. M.; Lund, C. R. F. *Catal. Lett.* **2001**, *73*, 73.
(8) Kogel, M.; Abu-Zied, B. M.; Schwefer, M.; Turek, T. *Catal. Commun.* **2001**, *2*, 273.
(9) Boutarbouch, M. N. D.; Cortes, J. M. G.; El Begrani, M. S.; de Lecea, C. S. M.; Perez-Ramirez, J. *Appl. Catal. B-Environ.* **2004**, *54*, 115.
(10) Sang, C. M.; Kim, B. H.; Lund, C. R. F. *J. Phys. Chem. B* **2005**, *109*, 2295.
(11) Kiwi-Minsker, L.; Bulushev, D. A.; Renken, A. *Catal. Today* **2005**, *110*, 191.
(12) Panov, G. I.; Sobolev, V. I.; Kharitonov, A. S. *J. Mol. Catal.* **1990**, *61*, 85.
(13) Dubkov, K. A.; Paukshtis, E. A.; Panov, G. I. *Kinet. Catal.* **2001**, *42*, 205.
(14) El-Malki, E. M.; van Santen, R. A.; Sachtler, W. M. H. *J. Catal.* **2000**, *196*, 212.
(15) Mauvezin, M.; Delahay, G.; Coq, B.; Kieger, S.; Jumas, J. C.; Olivier-Fourcade, J. *J. Phys. Chem. B* **2001**, *105*, 928.
(16) Grubert, G.; Hudson, M. J.; Joyner, R. W.; Stockenhuber, M. *J. Catal.* **2000**, *196*, 126.
(17) Turek, T. *Catal. Today* **2005**, *105*, 275.
(18) Bulushev, D. A.; Renken, A.; Kiwi-Minsker, L. *J. Phys. Chem. B* **2006**, *110*, 305.
(19) Lobree, L. J.; Hwang, I. C.; Reimer, J. A.; Bell, A. T. *Catal. Lett.* **1999**, *63*, 233.
(20) Mul, G.; Perez-Ramirez, J.; Kapteijn, F.; Moulijn, J. A. *Catal. Lett.* **2002**, *80*, 129.
(21) Yuranov, I.; Bulushev, D. A.; Renken, A.; Kiwi-Minsker, L. *J. Catal.* **2004**, *227*, 138.
(22) Kiwi-Minsker, L.; Bulushev, D. A.; Renken, A. *Catal. Today* **2004**, *91*−*92*, 165.
(23) Kiwi-Minsker, L.; Bulushev, D. A.; Renken, A. *J. Catal.* **2003**, *219*, 273.
(24) Bulushev, D. A.; Kiwi-Minsker, L.; Renken, A. *Catal. Today* **2000**, *57*, 231.
(25) Wood, B. R.; Reimer, J. A.; Bell, A. T.; Janicke, M. T.; Ott, K. C. *J. Catal.* **2004**, *224*, 148.
(26) Hadjivanov, K. I. *Catal. Rev.*−*Sci. Engl* **2000**, *42*, 71.
(27) Hensen, E. J. M.; Zhu, Q.; van Santen, R. A. *J. Catal.* **2003**, *220*, 260.
(28) Chen, H. Y.; Voskoboinikov, T.; Sachtler, W. M. H. *J. Catal.* **1998**, *180*, 171.
(29) Heyden, A.; Peters, B.; Bell, A. T.; Keil, F. J. *J. Phys. Chem. B* **2005**, *109*, 1857.
(30) Perez-Ramirez, J. *J. Catal.* **2004**, *227*, 512.
(31) Choi, S. H.; Wood, B. R.; Bell, A. T.; Janicke, M. T.; Ott, K. C. *J. Phys. Chem. B* **2004**, *108*, 8970.
(32) Dubkov, K. A.; Ovanesyan, N. S.; Shteinman, A. A.; Starokon, E. V.; Panov, G. I. *J. Catal.* **2002**, *207*, 341.
(33) Yakovlev, A. L.; Zhidomirov, G. M.; van Santen, R. A. *J. Phys. Chem. B* **2001**, *105*, 12297.
(34) Mul, G.; Zandbergen, M. W.; Kapteijn, F.; Moulijn, J. A.; Perez-Ramirez, J. *Catal. Lett.* **2004**, *93*, 113.
(35) Hensen, E. J. M.; Zhu, Q.; van Santen, R. A. *J. Catal.* **2005**, *233*, 136.
(36) Malykhin, S.; Zilberberg, I.; Zhidomirov, G. M. *Chem. Phys. Lett.* **2005**, *414*, 434.
(37) Moden, B.; Da Costa, P.; Lee, D. K.; Iglesia, E. *J. Phys. Chem. B* **2002**, *106*, 9633.
(38) Sang, C. M.; Lund, C. R. F. *Catal. Lett.* **2000**, *70*, 165.